

# High-frequency dielectric relaxation of liquid crystals: THz time-domain spectroscopy of liquid crystal colloids

Masahito Oh-e, Hiroshi Yokoyama

Liquid Crystal Nano-system Project, ERATO/SORST,  
Japan Science & Technology Agency,  
5-9-9 Tokodai, Tsukuba, Ibaraki-ken 300-2635 Japan  
[oh-e@nanolc.jst.go.jp](mailto:oh-e@nanolc.jst.go.jp), [yokoyama-hiroshi@aist.go.jp](mailto:yokoyama-hiroshi@aist.go.jp)

Mattijs Koeberg, Euan Hendry, Mischa Bonn

FOM Institute for Atomic and Molecular Physics,  
Kruislaan 407, 1098 SJ, Amsterdam, The Netherlands  
[mattijs@mac.com](mailto:mattijs@mac.com), [E.Hendry@exeter.ac.uk](mailto:E.Hendry@exeter.ac.uk), [bonn@amolf.nl](mailto:bonn@amolf.nl)

**Abstract:** Terahertz time-domain spectroscopy has been used to study the dielectric relaxation of pure 4'-n-pentyl-4-cyanobiphenyl (5CB) liquid crystal (LC) and its mixtures with 10  $\mu\text{m}$   $\text{SiO}_2$  particles in the frequency range 0.2–2 THz. For the pure sample, we find that spatial inhomogeneities consisting of oriented domains, comparable in size to our probe area ( $\sim 1 \text{ mm}^2$ ), cause a large scatter in the measured dielectric function, due to varying contributions from the ordinary and extraordinary components. In the LC/particle mixtures, ordering of the LC at the surface of the  $\text{SiO}_2$  particles results in a break-up of these domains, giving rise to a spatially much more homogeneous dielectric response. The inferred dielectric function can be interpreted using effective medium theory and the Debye relaxation model. We observe this stabilizing effect for interparticle distances  $< \sim 30 \mu\text{m}$ , setting a lower limit for the size of oriented domains in the bulk LC.

© 2006 Optical Society of America

**OCIS codes:** (300.6250) Spectroscopy, condensed matter; (300.6270) Spectroscopy, far infrared; (320.7150) Ultrafast spectroscopy; (160.3710) Liquid crystals; (160.6030) Silica.

---

## References and links

1. W. B. Russel, D. H. Saville, and W. R. Schowalter, *Colloidal Dispersions* (Cambridge University Press, Cambridge, 1991).
2. P. S. Drzaic, *Liquid Crystal Dispersions*, Series on Liquid Crystals (World Scientific, Singapore, 1995), Vol. 1.
3. P. Poulin, H. Stark, T. C. Lubensky, and D. A. Weitz, "Novel Colloidal Interactions in Anisotropic Fluids," *Science* **275**, 1770–1773 (1997).
4. T. C. Lubensky, D. Pettey, N. Currier, and H. Stark, "Topological defects and interactions in nematic emulsions," *Phys. Rev. E* **57**, 610–625 (1998).
5. P. Poulin and D. A. Weitz, "Inverted and multiple nematic emulsions," *Phys. Rev. E* **57**, 626–637 (1998).
6. P. G. de Gennes and J. Prost, *The Physics of Liquid Crystals* (Oxford University Press, London, 1993).
7. M. P. van Exter, Ch. Fattinger, D. Grischkowsky, "Terahertz time-domain spectroscopy of water vapor," *Opt. Lett.* **14**, 1128–1130 (1989).
8. D. Grischkowsky, S. Keiding, M. P. van Exter, and Ch. Fattinger, "Far-infrared time-domain spectroscopy with terahertz beams of dielectrics and semiconductors;" *J. Opt. Soc. Am. B* **7**, 2006–2015 (1990); E. Knoesel, M. Bonn, J. Shan, and T. F. Heinz, "Charge transport and carrier dynamics in liquids probed by THz time-domain spectroscopy," *Phys. Rev. Lett.* **86**, 340–343 (2001).

9. M. C. Beard, G. M. Turner, and C. A. Schmuttenmaer, "Terahertz Spectroscopy," *J. Phys. Chem. B* **106**, 7146–7159 (2002); J. Shan, F. Wang, E. Knoesel, M. Bonn, and T. F. Heinz, "Measurement of the Frequency-Dependent Conductivity in Sapphire," *Phys. Rev. Lett.* **90**, 247401 (2003); E. Hendry, J. M. Schins, L. P. Candeias, L. D. A. Siebbeles, and M. Bonn, "Efficiency of Exciton and Charge Carrier Photogeneration in a Semiconducting Polymer," *Phys. Rev. Lett.* **92**, 196601 (2004); E. Hendry, F. Wang, J. Shan, T. F. Heinz, and M. Bonn, "Electron transport in TiO<sub>2</sub> probed by THz time-domain spectroscopy," *Phys. Rev. B* **69**, 081101 (2004).
10. C.-Y. Chen, T.-R. Tsai, C.-L. Pan, and R.-P. Pan, "Room temperature terahertz phase shifter based on magnetically controlled birefringence in liquid crystals," *Appl. Phys. Lett.* **83**, 4497–4499 (2003).
11. T. Nose, S. Sato, K. Mizuno, J. Bae, and T. Nozokido, "Refractive index of nematic liquid crystals in the submillimeter wave region," *Appl. Opt.* **36**, 6383–6387 (1997).
12. D. Turchinovich, P. Knobloch, G. Luessem, and M. Koch, "THz time-domain spectroscopy on 4-(trans-4'-pentylcyclohexyl)-benzotrill," in *Liquid Crystals V, Iam-Choon Khoo ed.*, Proc. SPIE **4463**, 65–70 (2001).
13. T.-R. Tsai, C.-Y. Chen, C.-L. Pan, R.-P. Pan, and X.-C. Zhang, "Terahertz time-domain spectroscopy studies of the optical constants of the nematic liquid crystal 5CB," *Appl. Opt.* **42**, 2372–2376 (2003).
14. C.-L. Pan, C.-F. Hsieh, R.-P. Pan, M. Tanaka, F. Miyamaru, M. Tani, and M. Hangyo, "Control of enhanced THz transmission through metallic hole arrays using nematic liquid crystal," *Opt. Express* **13**, 3921–3930 (2005).
15. E. Hendry, PhD thesis *Charge dynamics in novel semiconductors* (University of Amsterdam, Netherlands, 2005).
16. X. C. Zhang, Y. Jin, and X. F. Ma, "Coherent measurement of THz optical rectification from electro-optic crystals," *Appl. Phys. Lett.* **61**, 2764–2766 (1992).
17. A. Nahata, A. S. Weling, and T. F. Heinz, "A wideband coherent terahertz spectroscopy system using optical rectification and electro-optic sampling," *Appl. Phys. Lett.* **69**, 2321–2323 (1996).
18. P. C. M. Planken, H. K. Nienhuys, H. J. Bakker, and T. Wencelbach, *J. Opt. Soc. Am. B* **18**, 313–317 (2001).
19. M. Born and E. Wolf, *Principle of Optics*, 6th ed. (Pergamon, Oxford, 1980).
20. E. Hecht, *Optics*, 4th ed. (Benjamin Cummings, San Francisco, 2002).
21. L. DuVillaret, F. Garet, and J. Coutaz, "A reliable method for extraction of material parameters in terahertz time-domain spectroscopy," *IEEE J. Sel. Top. Quantum Electron.* **2**, 739–746 (1996).
22. C. A. Schmuttenmaer, "Exploring Dynamics in the Far-Infrared with Terahertz Spectroscopy," *Chem. Rev.* **104**, 1759–1779 (2004).
23. J. C. Maxwell-Garnett, *Philos. Trans. R. Soc. London* **A203**, 385 (1904).
24. A. Kirchner, K. Busch, and C.M. Soukoulis, "Transport properties of random arrays of dielectric cylinders," *Phys. Rev. B* **57**, 277–288 (1998).
25. G. A. Niklasson, C. G. Granqvist, and O. Hunderi, "Effective medium models for the optical properties of inhomogeneous materials," *Appl. Opt.* **20**, 26–30 (1981).
26. P. Debye *Polar Molecules*, (Dover, New York, 1929).
27. M. Xu, P. Firman, S. Petrucci, and E. M. Eyring, "Molecular dynamics of organic carbonate solutions from 50 ps to 10 fs," *J. Phys. Chem.* **97**, 3968–3973 (1993).
28. W. H. de Jue, *Physical Properties of Liquid Crystalline Materials* (Gordon and Breach, Science Publishers Inc., New York, 1980).
29. B. R. Ratna and R. Shashidhar, "Dielectric properties of 4'-n-alkyl-4-cyanobiphenyls in their nematic phases," *Pramana* **6**, 278–283 (1976).
30. D. Lippens, J. P. Parneix, and A. Chapoton, "Etude du 4 heptyl 4' cyanobiphenyl a partir de l'analyse de ses proprietes dielectriques," *J. de Physique* **38**, 1465–1471 (1977).
31. S.-T. Wu, C.-S. Wu, M. Warengghem, and M. Ismaili, *Opt. Eng.* **32**, 1775–1780 (1993).
32. G. P. Sinha and F. M. Aliev, "Dielectric spectroscopy of liquid crystals in smectic, nematic, and isotropic phases confined in random porous media," *Phys. Rev. E* **58**, 2001–2010 (1998).
33. J. Leys, G. Sinha, C. Glorieux, and J. Thoen, "Influence of nanosized confinements on 4-n-decyl-4'-cyanobiphenyl (10CB): A broadband dielectric study," *Phys. Rev. E* **71**, 051709 (2005).

## 1. Introduction

Colloidal particles dispersed in a liquid crystal (LC) host play an important role in LC nanotechnology [1, 2]. A particle immersed in a nematic LC phase can behave topologically as the core of an orientational defect. Recent research related to LC/colloid systems has focused on elucidating how particles induce topological defects and structures, and how the induced elastic distortion of an LC host can create novel inter-particle interactions and ordered structures [3, 4, 5]. But, in addition to the local effects a particle may have, one may also expect some of the bulk properties of an LC to change, since a single particle in an LC may have an ability to change the orientation of the adjacent LC molecules over relatively long range [6]. Here, we investigate such changes in bulk properties of an LC colloid system using THz

time-domain spectroscopy (THz-TDS). We show that the high-frequency (terahertz) dielectric response of LC/colloid mixtures is affected already at very low colloid concentrations, indicating that the LC/colloid mixture effectively becomes homogeneous at THz wavelengths for sufficiently small inter-particle distance.

THz time-domain spectroscopy (THz-TDS) has recently emerged as a powerful spectroscopic technique to measure simultaneously the real and imaginary parts of the complex dielectric function, or in other words, refractive index and absorption coefficient, in the THz frequency range [7, 8, 9]. Previous THz studies on LCs were motivated, on the one hand, by the notion that this frequency region is dominated by vibrations and rotations of large segments of a molecule and collective intermolecular vibrations, which determine molecular assembly and packing structures in these materials. On the other hand, there has been technological interest in the application of LCs as a phase shifter in the THz frequency range [10]. The ordinary and extraordinary dielectric functions of LCs such as 4-(*trans*-4'-pentylcyclohexyl)-benzoxonitrile and 4'-*n*-pentyl-4-cyanobiphenyl at THz frequencies were previously determined using an LC confined cell [11, 12, 13, 14].

This letter reports the first THz-TDS transmission measurements on LC colloids. We compare spectra (in the frequency range 0.2–2.0 THz) for a pure nematic LC with and without a magnetic field, and with LC in which silica particles are dispersed. We find that sample inhomogeneities (presumably caused by oriented domains comparable in size to our probe area) cause a large spread in the observed dielectric response in the pure LC sample, while in the LC/particle mixtures, local ordering of the LC domains by the SiO<sub>2</sub> particles gives rise to a much more homogeneous dielectric response, which we interpret by combining effective medium theory with the Debye relaxation model. By varying the particle volume fraction from 0.5 to 10 %, we also show that the dielectric response of LC/colloid mixtures is affected already at very low particle concentrations, indicating that the LC/colloid mixture becomes homogeneous at THz wavelengths ( $\sim 100 \mu\text{m}$ ) when the average distance between particles is  $< 30 \sim 40 \mu\text{m}$ , indicating that this is the approximate size of oriented domains in the bulk LC.

## 2. Experimental

The THz-TDS setup has been described in detail elsewhere [9, 15]. Briefly, in this experiment, we use a Coherent Legend regenerative amplifier (Regen) seeded by a Coherent Vitesse and pumped by a Coherent Evolution. The amplified pulses are centered around 800 nm, have a temporal FWHM 120 fs and a 1 kHz repetition rate. Of the 2.5 W output power of the Regen, 90 mW is sufficient to run the spectrometer. THz pulses are generated in a phase-matched  $\langle 110 \rangle$  oriented zinc telluride (ZnTe) crystal through optical rectification [16, 17] using 80 mW of the Regen output. Generated THz pulses are collimated and then weakly focused onto a sample using a pair of rhodium-coated off-axis parabolic mirrors (focal length 11.9 cm). THz pulses transmitted through the sample are re-collimated and focused onto a second ZnTe detection crystal using a second pair of paraboloids. The strength of the THz field imaged onto the sampling crystal is detected through electro-optical sampling [18] using 5 mW of the Regen output. The setup is purged with dry nitrogen gas to eliminate absorption by water vapour.

The nematic LC used in this study is 4'-*n*-pentyl-4-cyanobiphenyl (5CB) from Merck Japan. Figure 1 shows the chemical structure of 5CB. THz transmission is measured through a 2 mm thick fused-quartz cuvette with no surface treatment, used to contain 5CB and its colloids. For the LC colloids, silica (SiO<sub>2</sub>) particles with 10  $\mu\text{m}$  diameter from micromod Partikeltechnologie GmbH are dispersed in 5CB as a function of volume fraction. The mixture is appropriately shaken and sonicated before each measurement to uniformly mix the particles in 5CB, and the measurement is carried out before the particles precipitate. A magnetic field is applied to LCs with a Nd magnet to measure uniaxially oriented the LC molecules. The

magnetic field at the center is 250 mT, which is sufficient to align the LC molecules in a 2 mm thick cuvette [10].

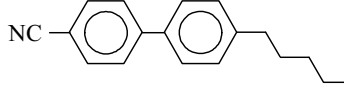


Fig. 1. Chemical structure of 5CB.

### 3. Analysis

In a THz–TDS measurement, a pulse of THz radiation passes through a sample and has its temporal profile changed compared to that of a reference pulse. THz pulses are essentially single cycle electromagnetic pulses with a period of  $\sim 1$  ps of which the transmitted field strength is detected directly in the time domain. The transmission of these pulses through the cuvette with and without a sample,  $E_{trans}(t)$  and  $E_{ref}(t)$  respectively, is recorded. The magnitude of the field and its time delay contain the information of the absorption and refraction, respectively, and hence the dielectric function. Through analysis in the frequency domain, the frequency dependent response of the material can be obtained. This response can be described in terms of the frequency dependent complex dielectric function. In our experiments using a 2 mm cuvette, a 5CB layer referred to as medium 2 is sandwiched between two fused-quartz substrates referred to as media 1 and 3. Here we can assume a three layer model, where the THz electric field that transmits from the medium 1 to 3 is given by [19, 20]:

$$E_{trans}(\omega) = t_{12}t_{23}\exp(i\sqrt{\epsilon_2}\omega d/c)E(\omega), \quad (1)$$

where  $E(\omega)$  is the Fourier transform of the THz wave just before exciting the first cuvette window,  $t_{ij}=2\sqrt{\epsilon_i}/(\sqrt{\epsilon_i}+\sqrt{\epsilon_j})$  is the transmission coefficient from medium  $i$  to medium  $j$  with  $\epsilon_i$  being the dielectric function in medium  $i$ , and  $\exp(i\sqrt{\epsilon_2}\omega d/c)$  is a function describing the propagation of the pulse in medium 2 with the thickness  $d$ , the angular frequency  $\omega$ , the light speed in vacuum  $c$  and the complex dielectric function  $\epsilon_2$ . Here the effect of multiple reflections is not included since  $d$  is large enough in our measurements to temporally separate reflections from the main pulse. Knowing that the electric field of the THz wave through an empty cuvette is described by  $E_{ref}(\omega) = t_{1air}t_{air3}\exp(i\omega d/c)E(\omega)$ , the difference in transmission for the sample and an empty cell,  $\Delta E$ , divided by  $E_{ref}$ , is given by

$$\begin{aligned} \frac{\Delta E(\omega)}{E_{ref}(\omega)} &= \frac{E_{trans}(\omega) - E_{ref}(\omega)}{E_{ref}(\omega)} \\ &= \frac{t_{12}t_{23}\exp(i\sqrt{\epsilon_2}\omega d/c)}{t_{1air}t_{air3}\exp(i\omega d/c)} - 1. \end{aligned} \quad (2)$$

In our analysis we used  $\epsilon_1=\epsilon_3=3.80$  for the dielectric constant of the windows of the fused-quartz cuvette [8, 13]. Numerical analysis of Eq.(2) allows us to quantitatively extract the complex dielectric function  $\epsilon_2(\omega)$ , containing the optical functions of the refractive index  $n(\omega)=\text{Re}[\sqrt{\epsilon_2}(\omega)]$  and the extinction coefficient  $k(\omega)=\text{Im}[\sqrt{\epsilon_2}(\omega)]$  of our sample [21, 22].

#### 4. Results and Discussion

Shown in Fig. 2(a) are the THz waveforms transmitted through the cuvette with and without 5CB under an applied magnetic field, and the real  $\text{Re}(\varepsilon)=\varepsilon'-n^2-k^2$  and imaginary  $\text{Im}(\varepsilon)=\varepsilon''=2nk$  parts of dielectric function deduced by the analysis mentioned above. The magnetic field is applied horizontally, i.e., in the direction parallel to the cuvette surface at  $\theta = 90^\circ$ , and hence the LC molecules are oriented in the same direction of the polarization of the incoming THz pulse. In a uniaxially anisotropic medium, the sample possesses extraordinary ( $\varepsilon_e$ ) and ordinary ( $\varepsilon_o$ ) dielectric functions. In our experimental geometry, the effective dielectric function  $\varepsilon$  is given by  $\varepsilon(\theta) = \varepsilon_e \varepsilon_o / (\varepsilon_o \sin^2 \theta + \varepsilon_e \cos^2 \theta)$ , where  $\theta$  is defined as the angle between the THz propagation direction and the magnetic field (equivalent to the molecular axis). At  $\theta = 90^\circ$  (Fig. 2(a)) the generated phase comes from  $\sqrt{\varepsilon_e}$  since the polarization of the THz wave coincides with the molecular orientation. Figure 2(b) displays the values of  $\varepsilon'(\omega)=\text{Re}[\varepsilon(\omega)]$  as a function of  $\theta$  at several THz frequencies. Here only the magnet is rotated horizontally with the cuvette being fixed. As expected, as the direction of the magnetic field is rotated azimuthally, the values of  $\varepsilon$  decrease, tending towards the value of  $\varepsilon_o$  as the molecules follow the magnetic field. These measurements under applied magnetic field are reproducible within 1% accuracy and the values of  $\varepsilon'$  can be extracted reliably. Solid lines are fits by the function  $\varepsilon(\theta)$  and these provide us with the inferred values of  $\varepsilon'_o$  and  $\varepsilon'_e$ , under a magnetic field, which are plotted in Fig. 5 for later discussion.

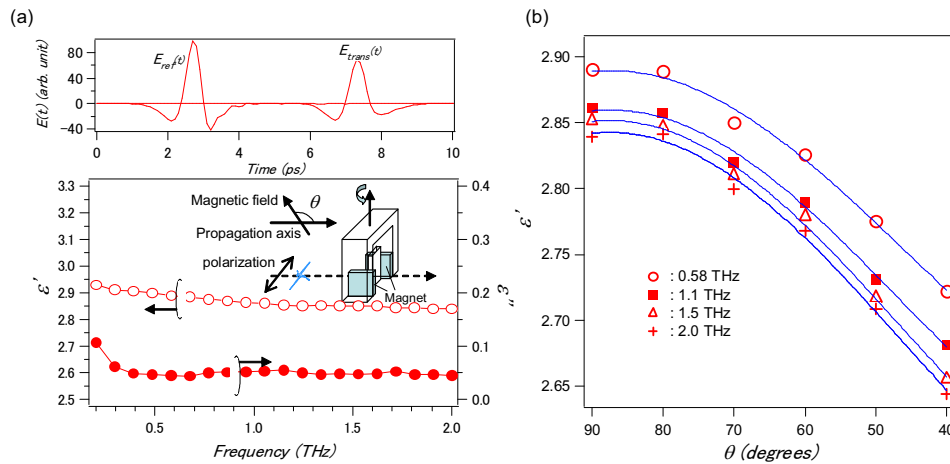


Fig. 2. (a) THz waveforms transmitted through the cuvette with and without the uniaxially oriented 5CB layer under a magnetic field,  $E_{trans}(t)$  and  $E_{ref}(t)$ , and  $\varepsilon'(\omega)$  and  $\varepsilon''(\omega)$  deduced from the obtained THz waveforms with  $\theta = 90^\circ$ . (b) Extracted  $\varepsilon'(\omega)$  as a function of the rotation angle  $\theta$  of a magnetic field. Solid lines are fits described in the text.

In the absence of the magnetic field, however, we notice that the THz waveforms through the randomly oriented 5CB layer suffer from a considerably lower reproducibility, and strong fluctuations in the derived  $\varepsilon'$  are observed (from  $\sim 2.55$  to  $\sim 2.85$  at 1.0 THz), with a spread in the extracted  $\varepsilon'(\omega)$  around 5%, i.e. significantly larger than the experimental sensitivity. The non-reproducible THz waveforms through the 5CB layer can be understood by considering the inhomogeneity of the sample in the absence of an externally applied magnetic field: as the cuvette surface is untreated, there is expected to be no preferential alignment of LC molecules in the bulk of the sample. Evidently, in such an unperturbed system, oriented domains self-organize with a size comparable to the THz beam of around  $\sim 1$  mm, resulting in the different

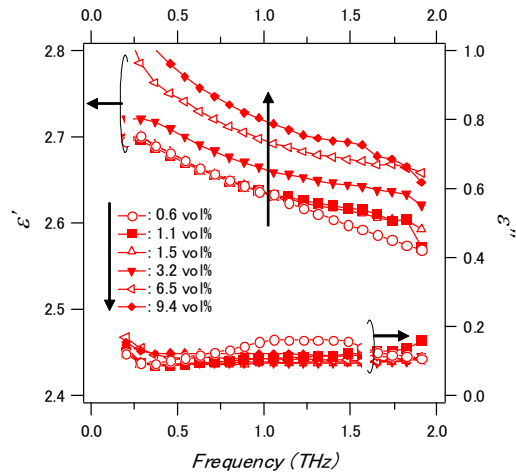


Fig. 3. Extracted dielectric functions, the real  $\epsilon'(\omega)$  and imaginary  $\epsilon''(\omega)$  parts, of the LC colloids as a function of SiO<sub>2</sub> particle volume fraction.

effective dielectric responses observed for different measuring spots.

Local symmetry breaking is therefore interesting, as it allows the reduction in the size of the different domains to well below both the spot size and the wavelength of the THz light, allowing the reliable determination of the effective dielectric response of the medium. Here, we use SiO<sub>2</sub> particles to cause symmetry breaking. Figure 3 shows  $\text{Re}(\epsilon)=\epsilon'=n^2-k^2$  and  $\text{Im}(\epsilon)=\epsilon''=2nk$  deduced from the measurements of LC colloids as a function of the particle volume fraction. At small volume fractions of the SiO<sub>2</sub> particles (0.6 % and 1.5 %) we observe an unvarying  $\epsilon'$ . For higher volume fractions,  $\epsilon'$  clearly increases as a function of increasing volume fraction. This behavior can qualitatively be understood as the adding-up effect of higher  $\epsilon'$  of SiO<sub>2</sub> compared to 5CB: the values of  $\epsilon'$  of the LC colloids should be between those of the pure 5CB and SiO<sub>2</sub>. We also notice that for a particle volume fraction exceeding 1.5 %, the effect of sample inhomogeneities is significantly reduced. The extracted  $\epsilon$  for fractions less than 1.5 % have a larger  $\sim 3\text{--}4\%$  inaccuracy, comparable to that observed for the unperturbed 5CB. At particle fractions above 1.5 %, the scatter lies again within 1 %. This implies that SiO<sub>2</sub> particles introduced in the 5CB have a capability to break up the LC domains and homogenize the medium on the lengthscale of the THz focus and wavelengths. The average particle spacing  $L$  in the colloids can be estimated from the volume fraction  $\alpha_d$  and the diameter of particle  $D$  with  $\alpha_d=\pi D^3/6L^3$ . For the threshold particle volume observed for these effects ( $\alpha_d = 1.1 \sim 1.5\%$ ),  $L$  can roughly be estimated as  $30 \sim 40 \mu\text{m}$ . This means that the LC/colloid mixture effectively becomes homogeneous at THz wavelengths ( $\sim 100 \mu\text{m}$ ) as long as the average distance between the particles is less than  $30 \sim 40 \mu\text{m}$ , suggesting an upper limit for the size of oriented domains in the bulk LC.

Since the LC colloids are an inhomogeneous mix of 5CB and SiO<sub>2</sub> particle regions, effective medium theory can be used to extract the dielectric properties of 5CB from the sample. To extract the effective dielectric function  $\epsilon$  of a medium consisting of non-interacting spherical particles with dielectric function  $\epsilon_p$  embedded within a medium  $\epsilon_m$ , we use Maxwell-Garnett(MG) theory, which reads [23, 24]:

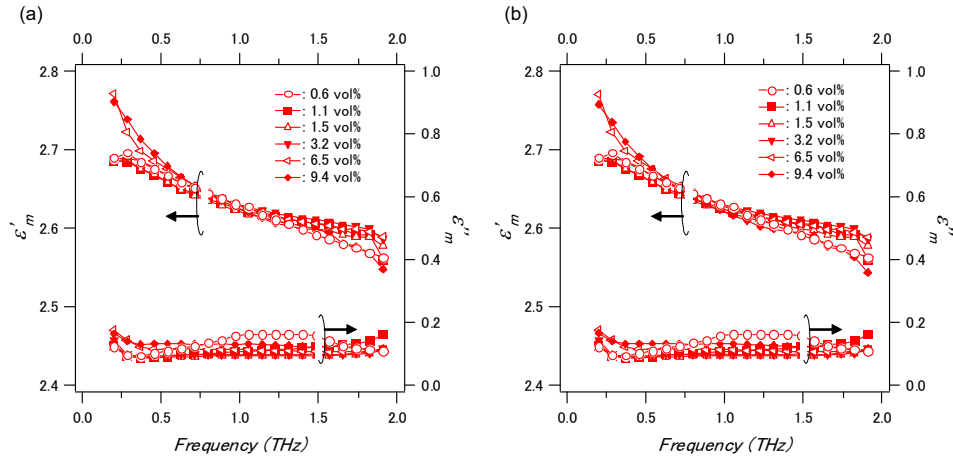


Fig. 4. Dielectric functions, the real  $\epsilon'_m(\omega)$  and imaginary  $\epsilon''_m(\omega)$  parts, of the 5CB media  $\epsilon_m$  extracted using (a)Maxwell-Garnett and (b)Bruggeman theories as a function of SiO<sub>2</sub> particle volume fraction.

$$\frac{\epsilon - \epsilon_m}{\epsilon + 2\epsilon_m} = s \frac{\epsilon_p - \epsilon_m}{\epsilon_p + 2\epsilon_m}, \quad (3)$$

where  $s$  is the space filling factor. MG theory describes a system where the particles  $\epsilon_p$  are dispersed in a continuous host of material  $\epsilon_m$  like a separated-grain structure [25]. This theory is valid only for low  $s$  ( $s < 0.15$ ), as it neglects polarization coupling between particles. Since  $s$  is lower than 0.1 in our measurements with the particle spacing  $L$  typically more than  $\sim 10 \mu\text{m}$ , MG theory is applicable. It should be noted that we obtain essentially identical results using other effective medium theories, such as Bruggeman's (BR) effective medium theory [23, 24].

From Eqs.(3) with  $\epsilon_p=3.8$  and  $\epsilon$  obtained in Fig. 3,  $\epsilon_m$  can be extracted for the corresponding  $s$ . Note that  $\epsilon_m$  is the dielectric function of randomly oriented 5CB. Shown in Fig. 4(a) and (b) are the dielectric functions  $\epsilon_m(\omega)$  of 5CB extracted from each LC colloid sample with MG and BR theories. The most striking characteristic in the figure is that the extracted  $\epsilon_m(\omega)$  from each LC colloid sample is very similar, and equivalent to that obtained while measuring the pure 5CB. It may seem that higher values of  $\epsilon'_m$  appear below 0.5 THz for higher particle volume fractions, but we cannot definitively conclude this, given the noise level of our measurements. The insensitivity of the extracted dielectric function to particle concentration indicates that any change in the 5CB bulk properties by foreign particles is not pronounced in the THz frequency range. Hence using LC colloids allows us to deduce the optical functions of the pure LC in a more reproducible manner by increasing the homogeneity of the sample.

As mentioned above, in a uniaxial medium,  $\epsilon_m$  consists of the extraordinary  $\epsilon_m^e$  and ordinary  $\epsilon_m^o$  components with the relation of  $\epsilon_m = \epsilon_m^o + (\epsilon_m^e - \epsilon_m^o) \langle \cos^2 \theta \rangle$ . Here  $\langle \cos^2 \theta \rangle$  denotes the expectation value of  $\cos^2 \theta$  in thermal equilibrium, implying the average molecular orientation. For a randomly oriented medium  $\langle \cos^2 \theta \rangle = 1/3$ . Hence, since  $\epsilon_m^e$  can be determined independently by applying a magnetic field as shown in Fig. 2(a) and  $\epsilon_m$  is inferred using effective medium theory in Fig. 4, we can then determine all the dielectric function components. Figure 5 shows the dielectric function,  $\epsilon_m$  and  $\epsilon_m^e$  and  $\epsilon_m^o$  that contribute to  $\epsilon_m$ , along with the  $\epsilon'_o$  obtained from the data in Fig. 2(b) (under an applied field). The real part of  $\epsilon_m(\omega)$  is found

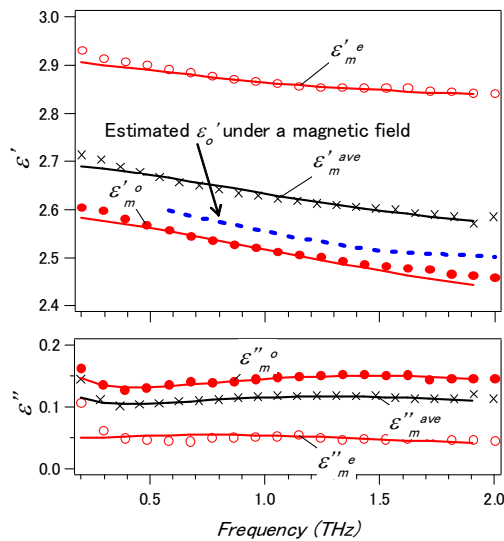


Fig. 5. Deduced dielectric functions, the real  $\epsilon'(\omega)$  and imaginary  $\epsilon''(\omega)$  parts, of the average  $\epsilon_m^{ave}$ , extraordinary  $\epsilon_m^e$  and ordinary  $\epsilon_m^o$  components of 5CB. Solid lines are fits to the deduced dielectric functions by a Debye expression. The dotted line represents  $\epsilon_o'$ , deduced from the measurement under a magnetic field shown in Fig. 2(b).

to decrease as a function of increasing frequency from 0.2–2 THz, while the imaginary part exhibits very small absorption in this range. This result is in marked contrast to ref.[13], which reports an *increase* of the THz refractive index (and thus the dielectric function) of 5CB with increasing frequency from 0.3–1.4 THz. Although we cannot elucidate the origin of this discrepancy, it may be traced to the nature of the sample in ref.[13]: a very thin LC cell of 25  $\mu\text{m}$  with a polyimide layer to align 5CB. One may expect transmission to be significantly affected by the interface for such very thin samples, giving rise to complications in the measurement. Additional complications could arise from a relatively large uncertainty in sample thickness for such a thin sample, as well as rubbing effects at the polymer surface. For the bulk (2 mm cuvette) samples reported here, these complications are circumvented.

The inferred  $\epsilon_o'$  under a magnetic field is slightly larger than  $\text{Re}[\epsilon_m^o]$  deduced from effective medium theory. Presumably this discrepancy originates from insufficient magnetic field strength to perfectly align the LC molecules against thermal disorder;  $\epsilon_o'$  therefore seems larger. This effect is expected to be much less important for  $\epsilon_e'$ , where the measurement is much less sensitive to the precise angle of the molecules (as is evident also from Fig. 2(b) around 90 deg).

Dielectric relaxation studies of polar liquids provide important information on molecular dipole dynamics [26, 27]. Generally, dielectric relaxation occurs via rotational relaxation of either the whole molecule or the flexible parts within the molecule. Such a relaxation of an oriented dipole in an alternating electric field is described by Debye relaxation. The dielectric response in the THz frequency regime may then be influenced by relaxations which occur nearby in frequency. Indeed, we can fit the dielectric function from Fig. 5 by a double Debye expression [28].

$$\epsilon(\omega) = \epsilon_\infty + \frac{\epsilon_0 - \epsilon_{int}}{1 - i\omega\tau_1} + \frac{\epsilon_{int} - \epsilon_\infty}{1 - i\omega\tau_2}, \quad (4)$$

where  $\epsilon_\infty$ ,  $\epsilon_0$ , and  $\epsilon_{int}$  denote the optical, the static, and the intermediate dielectric constants,



respectively, and  $\tau_1$  and  $\tau_2$  are relaxation time constants. The values that come out of the fit are as follows:  $\epsilon_\infty$ , 2.44;  $\epsilon_0$ , 9.5;  $\epsilon_{int}$ , 2.68;  $\tau_1$ ,  $\sim 56$  ps;  $\tau_2$ ,  $\sim 67$  fs. In the fit, the static dielectric constant is constrained to the known value [29, 30], while the fit result for the optical dielectric constant is reasonable [31]. We would like to note that the error in the inferred relaxation times is quite significant (reliable only to within a factor of  $\sim 2$ ), given the relatively small dispersion within our spectral window. Debye relaxation has recently been observed for the cyanobiphenyl LC in the GHz frequency range using broadband dielectric spectroscopy [32, 33]. These references support our results for the dispersion of the dielectric response, because the tail of the Debye relaxation, where the dielectric function decreases with increasing frequency, can be expected in the THz frequency range - precisely what we observe. The inferred relaxation times may be related to the relaxation of whole molecules or parts of molecules caused by the complex polar medium. However, the origin of the relaxation processes is yet to be confirmed.

## 5. Conclusion

In conclusion, we have shown that the LC bulk dielectric responses can be extracted from those of the LC colloids. The colloidal particles break the LC orientation domains, giving a very stable reproducible sample. We observe this stabilizing effect for interparticle distance  $< 40 \mu\text{m}$ , giving an approximate dimension for the size of oriented domains in the bulk LC. We are able, from our measurements on these colloids, to extract the optical functions of the bulk LC, suggesting that the orientational disorder that is induced by the colloids does not affect the dielectric relaxation of the 5CB molecules. The dielectric function is characterized by a decrease as a function of frequency from 0.2–2 THz with a relatively small absorption coefficient, in line with a Debye type response of the polar material.